Robotica (2001) volume 19, pp. 177–185. Printed in the United Kingdom © 2001 Cambridge University Press

Dynamic modeling and analysis of a two d.o.f. mobile manipulator

D. Naderi, A. Meghdari* and M. Durali

School of Mechanical Engineering, Sharif University of Technology, Tehran 11365–9567 (Iran).
E-mail: ameghdar@mines.edu

(Received in Final Form: September 12, 2000)

SUMMARY
This paper presents the kinematic and dynamic modeling of a two degrees of freedom manipulator attached to a vehicle with a two degrees of freedom suspension system. The vehicle is considered to move with a constant linear speed over an irregular ground-surface while the end-effector tracks a desired trajectory in a fixed reference frame. In addition, the effects of highly coupled dynamic interaction between the manipulator and vehicle (including the suspension system's effects) have been studied. Finally, simulation results for the end-effector's straight-line trajectory are presented to illustrate these effects.

KEYWORDS: Mobile manipulators; Kinematics & dynamics; Path following

I. INTRODUCTION

Performance requirements of civil and military operations in unstructured environments and urban terrain have motivated a different approach in handling of such missions using mobile manipulators. A manipulator mounted on a moving vehicle is called a *mobile manipulator.* A mobile manipulator with an appropriate suspension system can ride over uneven surfaces in unstructured environments and roads, and thus resulting in an expansion of its workspace. Additionally, if the manipulator could operate while the vehicle is traveling, the efficiency concerning with the time and energy used for stopping and starting will be increased.

Since the manipulator and vehicle dynamic equations are nonlinear, non-holonomic and highly coupled, deriving and solving the kinematic and dynamic equations of a mobile manipulator are rather complex. In order to isolate the manipulator from transmission of forces and displacements due to the ground-surface irregularities, a properly designed suspension system should be used. The suspension system affects the motion of the end effector both kinematically and dynamically. In the past several years, researchers in the field have shown an increasing interest in modeling and control of mobile manipulators. However, in most cases, effect of the suspension system in the model has been ignored. Therefore, the number of degrees of freedom of the vehicle is added to that of the corresponding manipulator, and the system is treated as a redundant manipulator. Nassal[1] has presented a coordination scheme called transparent coordination that allows for an arbitrary number of manipulators on a mobile platform and has introduced a collision avoidance scheme for two arm mobile robots. Dubowsky et al.[2] have developed a programming method in order to prevent the dynamic disturbances from going beyond the vehicles capacity, and hence maintain its stability while the manipulator is performing a speedy task. In addition, mobile manipulators are also meant to perform their prescribed tasks while going over uneven surfaces and maintaining their stability. A new tip-over stability margin for mobile manipulator which is easily computed and sensitive to top-heaviness, has been investigated by Papadopoulos et al.[3]. Chen et al.[4] presented an approach for the modeling and motion planning of a mobile manipulator system with a non-holonomic constraint. They used the Newton-Euler equations to obtain the complete dynamics of the system. The effects of the dynamic interaction between a manipulator and its mobile platform on the task performance has been studied by Yamamoto et al.[5] Pin et al.[6] have investigated the comparative trajectories involving combined motion of the platform and manipulator for problems with platform motion, to illustrate the use and efficiency of the FSP approach in complex motion planing problem. Carrikar et al.[7] considered the planning problem for a mobile manipulator system that must perform a sequence of tasks defined by position, orientation, force and moment vectors at the end effector. Lakota et al.[8] studied a manipulator having elastic elements and being mounted on a moving base. They used Lagrange equations and finite element method to derive the dynamic equations. Yamamoto et al.[9] investigated a coordinated task between a human and mobile manipulator in which the human operator takes an initiative of the task execution. Wang et al.[10] studied the velocity control of a manipulator mounted on a mobile base. One point to mention is that in all of the above works the effect of suspension system was not considered in the model.

Wilco et al.[11] considered a mobile robot equipped with soft spring suspension system. However the kinematic and dynamic equations of mobile robot have not been presented in their work. Tahboub[12,13] has considered a mobile

* Currently; Visiting Research Professor, Division of Engineering, Colorado School of Mines, Golden Colorado 80401-1888, USA, Email: ameghdar@mines.edu

https://doi.org/10.1017/S0263574700003131 Published online by Cambridge University Press

manipulator with suspension system. He has mentioned that neither the amplitude nor the pattern of base motion can be modeled accurately since it is a result of surface irregularities, vehicle jittery effects, and tracking errors. He has modeled the vehicle motion as an external disturbance. Meghdari et al.[14] presented the kinematic and dynamic modeling of a one degree of freedom manipulator attached to a vehicle with a two degrees of freedom suspension system.

In this paper, our objective is to present and analyze an exact kinematics and dynamics model of a two-degrees-of-freedom manipulator attached on a mobile platform with the suspension system, while traveling on an uneven surface.

II. KINEMATICS/DYNAMICS EQUATIONS OF A MOBILE MANIPULATOR

For the sake of modeling and analysis, a two-link planar manipulator attached on a two-degrees-of-freedom suspension system is considered. Figure 1 shows a simple schematics of such a system. The manipulator is attached to the moving base by a revolute joint, and the base is attached to weightless wheels by two linear springs and two linear dampers. Mass of each link is assumed to be concentrated at its mass center positioned at the middle of each link. The manipulator is held at its position via the torque's exerted by the corresponding actuators. Furthermore, a two-degrees-of-freedom vehicle sprung mass model is chosen for the vehicle model.[15]

In addition, it is assumed that the vehicle is moving on an uneven surface defined by a simple harmonic function with an amplitude of U_0 and the wavelength of λ, with the wheels and the surface remaining in contact at all times.

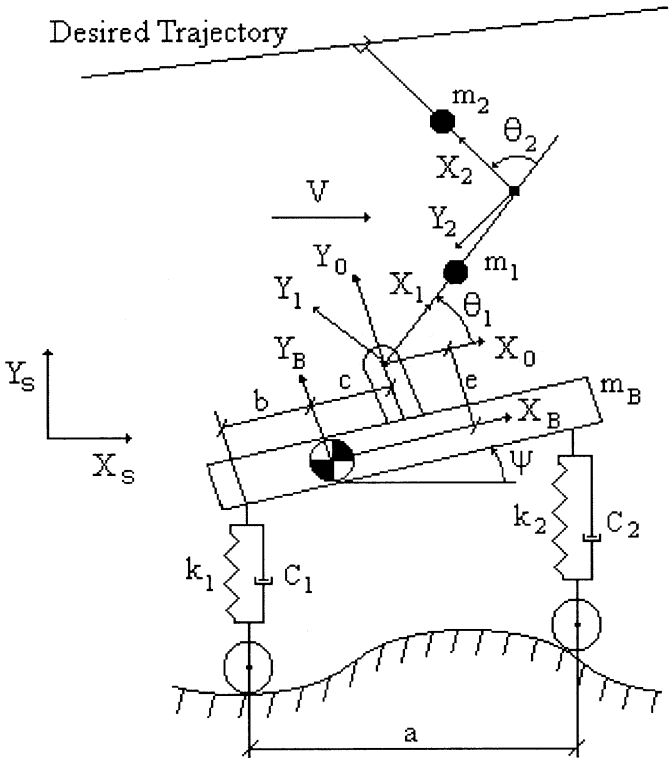

Fig. 1. Manipulator and vehicle model

Referring to the frames shown in Figure 1, one can readily define the homogenous transformation matrices as follows:[16]

$$ {}^{1}_{2}T = \begin{bmatrix} \cos\theta_2 & -\sin\theta_2 & 0 & \ell_1 \\ \sin\theta_2 & \cos\theta_2 & 0 & 0 \\ 0 & 0 & 1 & 0 \\ 0 & 0 & 0 & 1 \end{bmatrix} \quad {}^{1}_{2}R = \begin{bmatrix} \cos\theta_2 & -\sin\theta_2 & 0 \\ \sin\theta_2 & \cos\theta_2 & 0 \\ 0 & 0 & 1 \end{bmatrix} \tag{1} $$

$$ {}^{0}_{1}T = \begin{bmatrix} \cos\theta_1 & -\sin\theta_1 & 0 & 0 \\ \sin\theta_1 & \cos\theta_1 & 0 & 0 \\ 0 & 0 & 1 & 0 \\ 0 & 0 & 0 & 1 \end{bmatrix} \quad {}^{0}_{1}R = \begin{bmatrix} \cos\theta_1 & -\sin\theta_1 & 0 \\ \sin\theta_1 & \cos\theta_1 & 0 \\ 0 & 0 & 1 \end{bmatrix} \tag{2} $$

$$ {}^{B}_{0}T = \begin{bmatrix} 1 & 0 & 0 & c \\ 0 & 1 & 0 & e \\ 0 & 0 & 1 & 0 \\ 0 & 0 & 0 & 1 \end{bmatrix} \quad {}^{B}_{0}R = \begin{bmatrix} 1 & 0 & 0 \\ 0 & 1 & 0 \\ 0 & 0 & 1 \end{bmatrix} \tag{3} $$

$$ {}^{S}_{B}T = \begin{bmatrix} \cos\psi & -\sin\psi & 0 & vt \\ \sin\psi & \cos\psi & 0 & y \\ 0 & 0 & 1 & 0 \\ 0 & 0 & 0 & 10 \end{bmatrix} \quad {}^{S}_{B}R = \begin{bmatrix} \cos\psi & -\sin\psi & 0 \\ \sin\psi & \cos\psi & 0 \\ 0 & 0 & 1 \end{bmatrix} \tag{4} $$

Using the iterative Newton-Euler's dynamic algorithm,[16] the forces and torques at the joints of the manipulator can be evaluated. Since the manipulator is attached on a moving base with accelerations of $\ddot{y}$ and $\ddot{\psi}$, these accelerations are also accounted for in the dynamical equations similar to gravitational acceleration.

$$ {}^{1}P_{c_1} = l_1/2\hat{X}_1 \quad , \quad {}^{c_1}I_1 = 0 \quad , \quad {}^{2}P_{c_2} = l_2/2\hat{X}_2 \quad , \quad {}^{c_2}I_2 = 0 \tag{5} $$

$$ {}^{3}f_3 = 0 \quad , \quad {}^{3}n_3 = 0 \quad , \quad h = \sqrt{c^2 + e^2} \quad , \quad \gamma = \tan^{-2}(e/c) \tag{6} $$

$$ {}^{0}\omega_0 = \begin{bmatrix} 0 \\ 0 \\ \dot{\psi} \end{bmatrix}, \quad {}^{0}\dot{\omega}_0 = \begin{bmatrix} 0 \\ 0 \\ \ddot{\psi} \end{bmatrix}, $$

$$ {}^{0}\dot{v}_0 = \begin{bmatrix} -h\ddot{\psi}\sin\gamma - h\dot{\psi}^2\cos\gamma + (g+\ddot{y})\sin\psi \\ h\ddot{\psi}\cos\gamma - h\dot{\psi}^2\sin\gamma + (g+\ddot{y})\cos\psi \\ 0 \end{bmatrix} \tag{7} $$

The forces and the torque exerted to the vehicle by manipulator are obtained as follows (please see Appendix A for details):

$$ {}^{0}n_1 = \begin{bmatrix} 0 \\ 0 \\ \tau_1 \end{bmatrix} \tag{8} $$

https://doi.org/10.1017/S0263574700003131 Published online by Cambridge University Press

$$\tau_1 = 1/2m_2\ell_2(g+\ddot{y})\cos(\theta_1+\theta_2+\psi) + 1/2m_2\ell_2 h\ddot{\psi}\cos(\theta_1+\theta_2-\gamma) + 1/2\ell_1(m_1+2m_2)(g+\ddot{y})\cos(\theta_1+\psi) + 1/2\ell_1 h\ddot{\psi}(m_1+2m_2)\cos(\theta_1-\gamma) - 1/2\ell_1 h\dot{\psi}^2(m_1+2m_2)\sin(\theta_1-\gamma) - m_2\ell_1\ell_2(\dot{\theta}_1\dot{\theta}_2+1/2\dot{\theta}_2^2+\dot{\psi}\dot{\theta}_2)\sin\theta_2 + m_2\ell_1\ell_2(\ddot{\theta}_1+1/2\ddot{\theta}_2+\ddot{\psi})\cos\theta_2 + 1/2m_2\ell_2 h\dot{\psi}^2\sin(\theta_1+\theta_2-\gamma) + 1/4m_1\ell_1^2(\ddot{\theta}_1+\ddot{\psi}) + 1/4m_2\ell_2^2(\ddot{\theta}_1+\ddot{\theta}_2+\ddot{\psi}) + m_2\ell_1^2(\ddot{\theta}_1+\ddot{\psi}) \quad (9)$$

$${}^0f_0 = \begin{bmatrix} f_x \\ f_y \\ 0 \end{bmatrix} \quad (10)$$

$$f_x = -1/2m_2\ell_2(\dot{\theta}_1+\dot{\theta}_2+\dot{\psi})^2\cos(\theta_1+\theta_2) - 1/2m_2\ell_2(\ddot{\theta}_1+\ddot{\theta}_2+\ddot{\psi})\sin(\theta_1+\theta_2) - 1/2\ell_1(m_1+2m_2)(\dot{\theta}_1+\dot{\psi})^2\cos(\theta_1) - 1/2\ell_1(m_1+2m_2)(\ddot{\theta}_1+\ddot{\psi})\sin(\theta_1) + (m_1+m_2)(g+\ddot{y})\sin\psi - h\dot{\psi}^2(m_1+m_2)\cos\gamma - h\ddot{\psi}(m_1+m_2)\sin\gamma \quad (11)$$

$$f_x = -1/2m_2\ell_2(\dot{\theta}_1+\dot{\theta}_2+\dot{\psi})^2\sin(\theta_1+\theta_2) + 1/2m_2\ell_2(\ddot{\theta}_1+\ddot{\theta}_2+\ddot{\psi})\cos(\theta_1+\theta_2) - 1/2\ell_1(m_1+2m_2)(\dot{\theta}_1+\dot{\psi})^2\sin(\theta_1) + 1/2\ell_1(m_1+2m_2)(\ddot{\theta}_1+\ddot{\psi})\cos(\theta_1) + (m_1+m_2)(g+\ddot{y})\cos\psi - (m_1+m_2)h\dot{\psi}^2\sin\gamma + (m_1+m_2)h\ddot{\psi}\cos\gamma \quad (12)$$

III. DERIVING THE DYNAMICAL EQUATIONS OF THE VEHICLE

Identifying the forces and the torque applied on the vehicle by the manipulator, one can draw the free body diagram of the vehicle as shown in Figure 2. The driving torque is applied to the rear wheel. Applying Newton's Equations, we have:

$$\Sigma F_x = 0 \quad (13)$$

$$f = f_x\cos(\psi) - f_y\sin(\psi) \quad (14)$$

$$\Sigma F_y = m_B\ddot{y} \quad (15)$$

$$k_1(U_1(t)-y+b\psi)+c_1(\dot{U}_1(t)-\dot{y}+b\dot{\psi}) + k_2(U_2(t)-y-(a-b)\psi)+c_2(\dot{U}^2(t)-\dot{y} - (a-b)\dot{\psi}) - f_x\sin\psi - f_y\cos\psi = m_B\ddot{y} \quad (16)$$

Applying Euler's Equation we have:

$$\Sigma T = I_G\ddot{\psi} \quad (17)$$

$$fb\sin\psi - (k_1(U_1(t)-y+b\psi)+c_1(\dot{U}(t)-\dot{y}+b\dot{\psi}))b\cos\psi + (k_2(U_2(t)-y-(a-b)\psi)+c_2(\dot{U}_2(t)-\dot{y} - (a-b)\dot{\psi}))(a-b)\cos\psi + f_xe - f_yc - \tau_1 = I_G\ddot{\psi} \quad (18)$$

In the case where values of θ_1, $\dot{\theta}_1$, $\ddot{\theta}_1$, θ_2, $\dot{\theta}_2$ and $\ddot{\theta}_2$ are known as functions of time, the value of y and ψ can be computed by solving the differential equations (16) and (18).

IV. OBTAINING THE POSITION OF THE END EFFECTOR

Once the values of y and ψ are computed, the transformation matrix (4) will be known. Then one can evaluate the manipulator's tip position in frame {S} using the following relations:

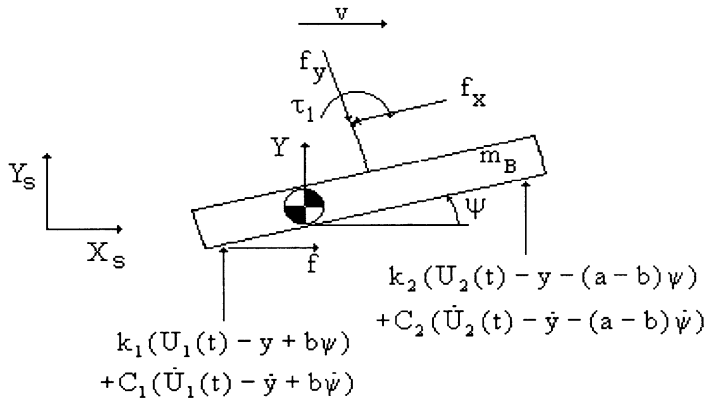

$$U_1(t) = U_0\cos(2\pi vt/\lambda) \quad , \quad U_2(t) = U_0\cos(2\pi vt/\lambda + 2\pi a/\lambda)$$

Fig. 2. Free body diagram of vehicle

https://doi.org/10.1017/S0263574700003131 Published online by Cambridge University Press

$$
{}^{s}\begin{bmatrix} X \\ Y \\ 0 \\ 1 \end{bmatrix} = \begin{bmatrix} \cos\psi & -\sin\psi & 0 & vt \\ \sin\psi & \cos\psi & 0 & y \\ 0 & 0 & 1 & 0 \\ 0 & 0 & 0 & 1 \end{bmatrix} \begin{bmatrix} 1 & 0 & 0 & c \\ 0 & 1 & 0 & e \\ 0 & 0 & 1 & 0 \\ 0 & 0 & 0 & 1 \end{bmatrix}
$$

$$
\begin{bmatrix} \cos\theta_1 & -\sin\theta_1 & 0 & 0 \\ \sin\theta_1 & \cos\theta_1 & 0 & 0 \\ 0 & 0 & 1 & 0 \\ 0 & 0 & 0 & 1 \end{bmatrix}
$$

$$
\begin{bmatrix} \cos\theta_2 & -\sin\theta_2 & 0 & \ell_1 \\ \sin\theta_2 & \cos\theta_2 & 0 & 0 \\ 0 & 0 & 1 & 0 \\ 0 & 0 & 0 & 1 \end{bmatrix}^{2} \begin{bmatrix} \ell_2 \\ 0 \\ 0 \\ 1 \end{bmatrix} \tag{19}
$$

$$
{}^{S}X = \ell_2 \cos(\psi + \theta_1 + \theta_2) + \ell_1 \cos(\psi + \theta_1) + c\cos\psi - e\sin\psi + vt \tag{20}
$$

$$
{}^{S}Y = \ell_2 \sin(\psi + \theta_1 + \theta_2) + \ell_1 \sin(\psi + \theta_1) + c\sin\psi - e\cos\psi + y \tag{21}
$$

V. END EFFECTOR'S POSITION FOR A STRAIGHT-LINE TRAJECTORY

It is obvious that to have a straight-line trajectory for the end effector in frame {S}, y and ψ must be functions of t, θ_1, $\dot{\theta}_1$, $\ddot{\theta}_1$, θ_2, $\dot{\theta}_2$ and $\ddot{\theta}_2$. In addition, θ_1 and θ_2 must also be functions of t, y, and ψ. Therefore, the differential equations (16) and (18) should convert to partial differential equations. To avoid this, the following numerical method is presented. If the end effector tracks a straight-line trajectory with a constant speed v_f, then equations (20) and (21) must satisfy the following relations:

$$
{}^{S}Y = \alpha\,{}^{S}X + \beta \tag{22}
$$

$$
{}^{s}X = v_f t \cos(\tan^{-1}\alpha) \tag{23}
$$

Where α and β are constants defining the desired trajectory. Substituting equations (20) and (21) into equations (22) and (23) results:

$$
\ell_2 \sin(\psi + \theta_1 + \theta_2) + \ell_1 \sin(\psi + \theta_1) + c\sin\psi + e\cos\psi + y = \alpha(\ell_2 \cos(\psi + \theta_1 + \theta_2) + \ell_1 \cos(\psi + \theta_1) + c\cos\psi - e\sin\psi + vt) + \beta \tag{24}
$$

$$
\ell_2 \cos(\psi + \theta_1 + \theta_2) + \ell_1 \cos(\psi + \theta_1) + c\cos\psi - e\sin\psi + vt = v_f t \cos(\tan^{-1}\alpha) \tag{25}
$$

Using the MAPLE software, differential equations (16), (18) and equations (24), (25) were solved numerically in accordance to the following conditions:

1. Values of $\dot{\theta}_1$, $\ddot{\theta}_1$, $\dot{\theta}_2$ and $\ddot{\theta}_2$ are considered to be zero.
2. Equations (16) and (18) are solved, and the value of y and ψ at $t = 0$ is computed.
3. Equations (24) and (25) are solved for $y(t = 0)$ and $\psi(t = 0)$, and θ_1 and θ_2 are then obtained.
4. Equations (16) and (18) are solved, and the value of y and ψ at $t = 0.01$ is computed.

Table I. Sample numerical values for model parameters.

$C_1 = 120$ N-s/m	$C_2 = 80$ N-s/m	$c = 0.2$ m	$e = 0.2$ m
$k_1 = 1200$ N/m	$k_2 = 800$ N/m	$\lambda = 0.3$ m	$v = 0.3$ m/s
$I_G = 2$ kg-m^2	$b = 0.4$ m	$a = 1$ m	$\ell_1 = 0.7$ m
$m_B = 20$ kg	$m_1 = 4$ kg	$U_0 = 0.03$ m	$v_f = 0.3$ m/s
$m_2 = 3$ kg	$\ell_2 = 0.7$ m		

5. Equations (24) and (25) are solved for $y(t = 0.01)$ and $\psi(t = 0.01)$, and θ_1 and θ_2 are then obtained.
6. Values of $\dot{\theta}_1$, $\ddot{\theta}_1$, $\dot{\theta}_2$ and $\ddot{\theta}_2$ are linearly estimated by the following relations:

$$
\dot{\theta}_1 = \frac{\theta_{1(new)} - \theta_{1(old)}}{0.01} \quad , \quad \ddot{\theta}_1 = \frac{\dot{\theta}_{1(new)} - \dot{\theta}_{1(old)}}{0.01} \quad ,
$$

$$
\dot{\theta}_2 = \frac{\theta_{2(new)} - \theta_{2(old)}}{0.01} \quad , \quad \ddot{\theta}_2 = \frac{\dot{\theta}_{2(new)} - \dot{\theta}_{2(old)}}{0.01}
$$

7. The above procedures are repeated from line 4 up, to the point where the error values for θ_1, $\dot{\theta}_1$, $\ddot{\theta}_1$, θ_2, $\dot{\theta}_2$ and $\ddot{\theta}_2$ are reduced to less than $\varepsilon = 0.01$.
8. By the above method, the values of y, ψ, θ_1 $\dot{\theta}_1$, $\ddot{\theta}_1$, θ_2, $\dot{\theta}_2$ and $\ddot{\theta}_2$ at $t = 0.01$ are computed. The procedure from line 4 to 7 is then iterated for other time steps.

VI. NUMERICAL RESULTS

The numerical parameters as shown in Table I are considered for the modeled mobile manipulator. To choose the parameters, the vehicle is considered without the manipulator. Then the parameters k_1, k_2, C_1, C_2, a and b are chosen such that the vehicle's differential equations of motion become uncoupled. For these parameters, the vehicle has two natural frequencies $f_{n1} = 1.592$ Hz and $f_{n2} = 2.466$ Hz. The values of vehicle speed corresponding to these natural frequencies are $v = 0.477$ m/s, and $v = 0.740$ m/s.

In the following examples, two typical trajectories are selected and the dynamic interaction between the vehicle and the manipulator are studied.

Example 1: The desired trajectory is a straight line with a zero slope at a vertical distance of 1.2 m from inertial reference frame {S}, (i.e. ${}^{S}Y = 1.2$ m or $\alpha = 0$, $\beta = 1.2$ m). To follow this trajectory, the differential equations (16), (18) and equations (24) and (25) are solved and the values of y, ψ, θ_1 and θ_2 are computed. These values are substituted into the equation (19) and the actual trajectory is plotted (Fig. 3). Figure 3 shows that the actual trajectory is nearly the same as the desired trajectory, thus the solving procedure is verified. The value of y with dynamic interaction effects (solid line) and without dynamic interaction effects (dashed line) are plotted in Figure 4. The down shift of the curve corresponding to the case with dynamic interaction effects is due to the fact that y reference is chosen as the static equilibrium position of vehicle alone, while in this case. The weight of the manipulator's links are present in forces and

https://doi.org/10.1017/S0263574700003131 Published online by Cambridge University Press

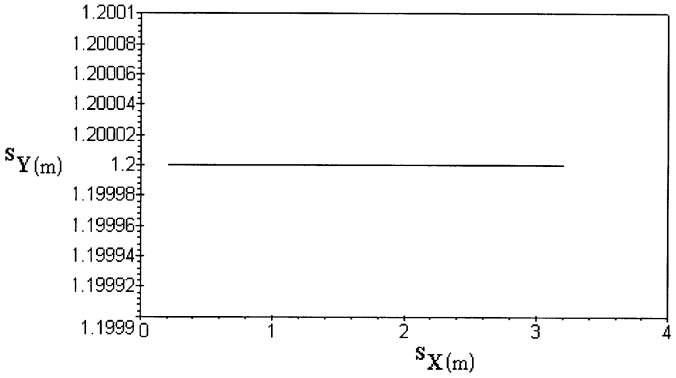

Fig. 3. End effector's trajectory

torque (f_x, f_y, τ_1). The amplitude of y increases about 65% in steady state response due to dynamic interaction effects. Since the dynamic interaction forces and torque exclude the $\dot{y}$ term, the phase is not changed. The time history of ψ, θ_1 and θ_2 without dynamic interaction effects (dashed-line) and with dynamic interaction effects (solid-line) are shown in Figures 5, 6 and 7. The amplitude of ψ, θ_1 and θ_2 increase about 23%, 62% and 142%, respectively, due to the dynamic interaction effects. The $(m_1 + m_2)g$, $m_2 g \ell_2/2$ and $\ell_1/2(m_1 + 2m_2)g$ terms in the dynamic interaction forces and torque (f_x, f_y, τ_1) result in a downshifting of the curve in Figure 5. The $\dot{\psi}$ terms in the dynamic interaction forces and

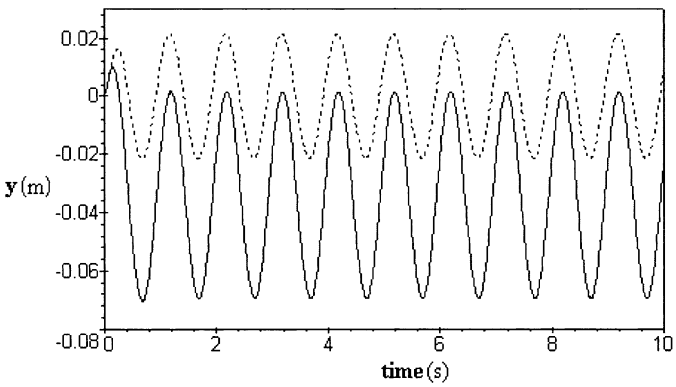

*__Dashed:__ Without dynamic interaction effects, __Solid:__ With dynamic interaction effects

Fig. 4. Variation of y versus time*

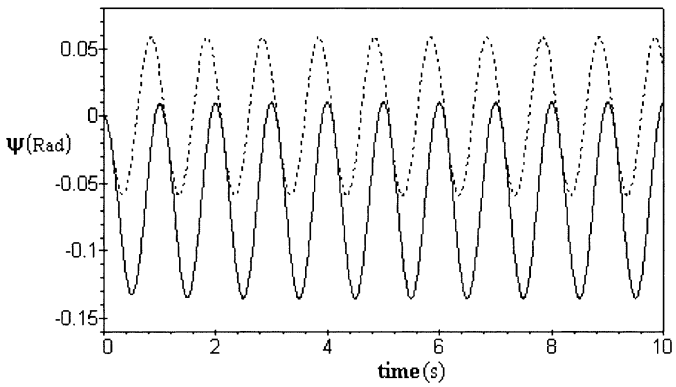

*__Dashed:__ Without dynamic interaction effects, __Solid:__ With dynamic interaction effects

Fig. 5. Variation of ψ versus time*

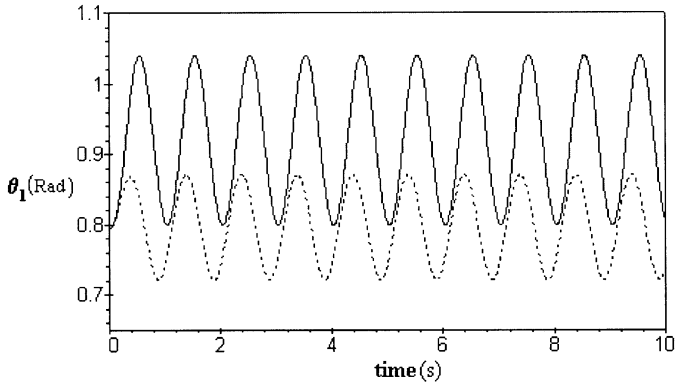

*__Dashed:__ Without dynamic interaction effects, __Solid:__ With dynamic interaction effects

Fig. 6. Variation of θ_1 versus time*

torque affect the phase angle of ψ, and change the value of the phase angle. This change leads to a similar change in θ_1. At the steady state response, the amplitude of y, ψ, θ_1 and θ_2 remain constant with respect to time. This means that after a time interval, the amplitudes of vibration approach to some constant values.

Example 2: The desired trajectory is a straight line with a 0.35 slope and at a vertical distance of 0.40 m from inertial reference frame {S}, (i.e. $^{S}Y = 0.35\ ^{S}X + 0.40$ m or $\alpha = 0.35$, $\beta = 0.40$ m). To follow this trajectory the differential equations (16), (18) and equations (24) and (25) are solved and the values of y, ψ, θ_1 and θ_2 are computed. These values are substituted into equation (19) and the actual trajectory is plotted (Fig. 8). Figure 8 shows that the actual trajectory is nearly the same as the desired trajectory. The time history of y, ψ, θ_1 and θ_2 with dynamic interaction effects (solid line) and without dynamic interaction effects (dashed line) are plotted in Figures 9, 10, 11 and 12. The amplitude of y decreases and the amplitude of ψ, θ_1 and θ_2 increases with respect to time due to dynamic interaction effects. The related discussion in example 1 is also valid for this example. Increasing amplitudes of ψ, θ_1 and θ_2 may cause the mobile manipulator to become unstable.

In example 1 the amplitude of y, ψ, θ_1 and θ_2 in the region of steady state response remains constant throughout the trajectory. Thus, this case is selected for investigating the dynamic interaction effects due to vehicle speed variations. The vehicle speed is varied from 0.05 m/s to 1 m/s. This

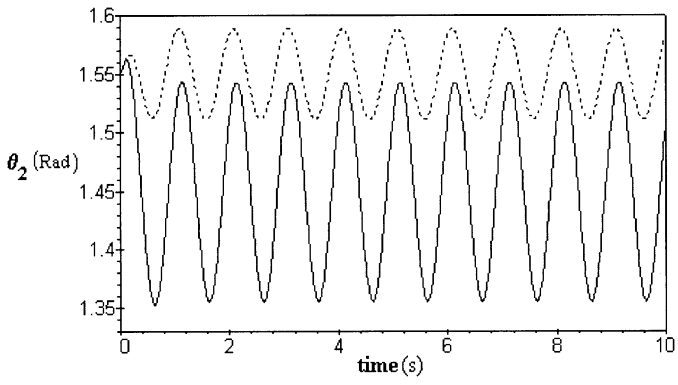

*__Dashed:__ Without dynamic interaction effects, __Solid:__ With dynamic interaction effects

Fig. 7. Variation of θ_2 versus time*

https://doi.org/10.1017/S0263574700003131 Published online by Cambridge University Press

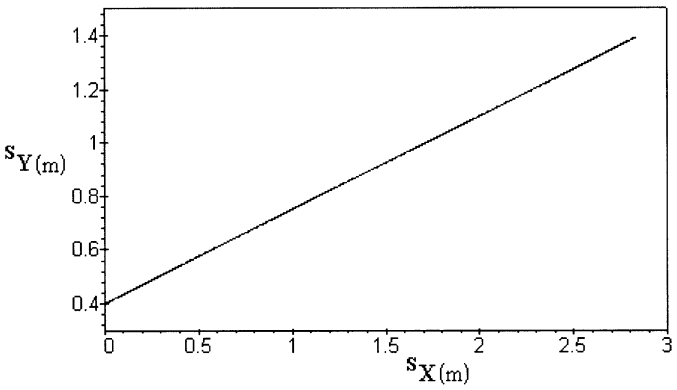

Fig. 8. End effector's trajectory

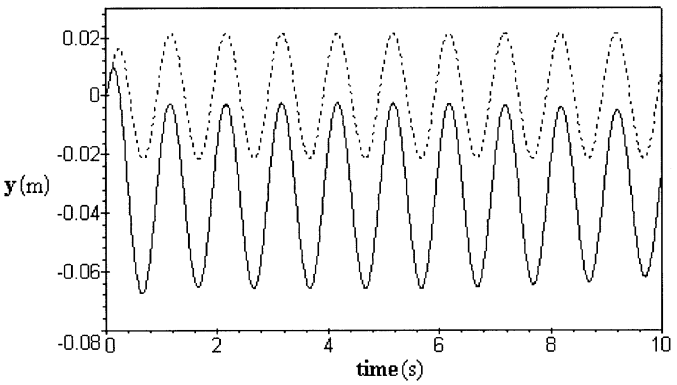

Fig. 9. Variation of y versus time*

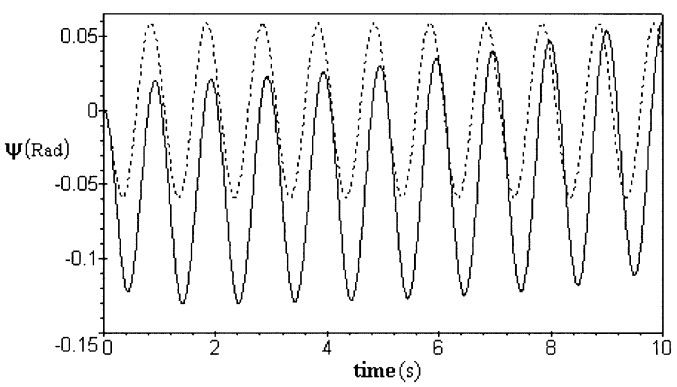

*Dashed: Without dynamic interaction effects, **Solid:** With dynamic interaction effects

Fig. 10. Variation of ϕ versus time*

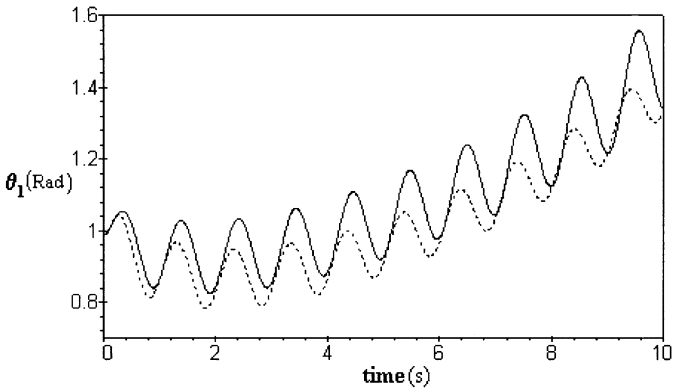

*Dashed: Without dynamic interaction effects, **Solid:** With dynamic interaction effects

Fig. 11. Variation of θ_1 versus time*

range includes the velocities (v = 0.477 m/s, v = 0.740 m/s) corresponding to the natural frequencies of the vehicle (f_{n1} = 1.592 Hz, f_{n2} = 2.466 Hz). The amplitudes of y, ψ, θ_1 and θ_2 with respect to vehicle speed with dynamic interaction effects (solid-line) and without dynamic interaction effects (dashed-line) are plotted in Figures 13, 14, 15 and 16. The amplitudes of y and ψ without dynamic interaction effects have one peck because the vehicle's differential equations of motion are uncoupled. It can be seen that, the dynamic interaction effects cause a considerable change in the amplitude of y, ψ, θ_1 and θ_2. The amplitude of y increases over the velocity range 0.05 m/s to 0.69 m/s and it decreases for the velocities higher than 0.69 m/s due to dynamic interaction effects. The amplitude of ψ increases over the velocity range 0.05 m/s to 0.33 m/s and it decreases for the velocities higher than 0.33 m/s due to dynamic interaction effects. The pick value of the amplitude of θ_1 and θ_2 increase and they are shifted to the lower velocity zone due to dynamic interaction effects. Thus, for reducing the amplitude of y and ψ it is recommended that the velocity of vehicle to be equal or greater than 0.69 m/s.

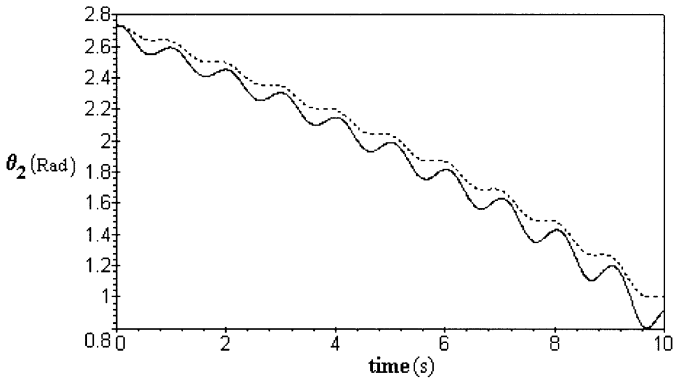

*Dashed: Without dynamic interaction effects, **Solid:** With dynamic interaction effects

Fig. 12. Variation of θ_2 versus time*

https://doi.org/10.1017/S0263574700003131 Published online by Cambridge University Press

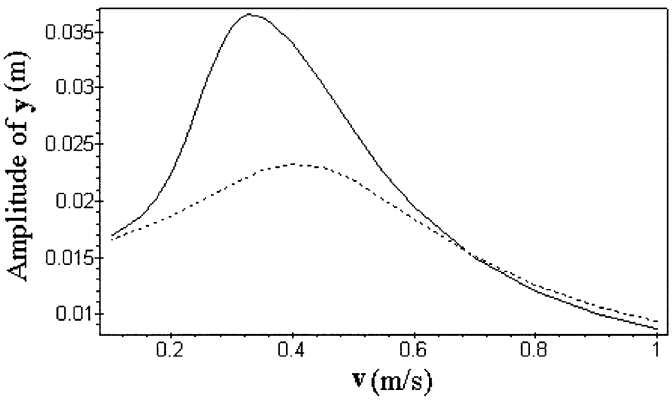

*Dashed: Without dynamic interaction effects, **Solid:** With dynamic interaction effects

Fig. 13. Amplitude of y versus velocity of vehicle*

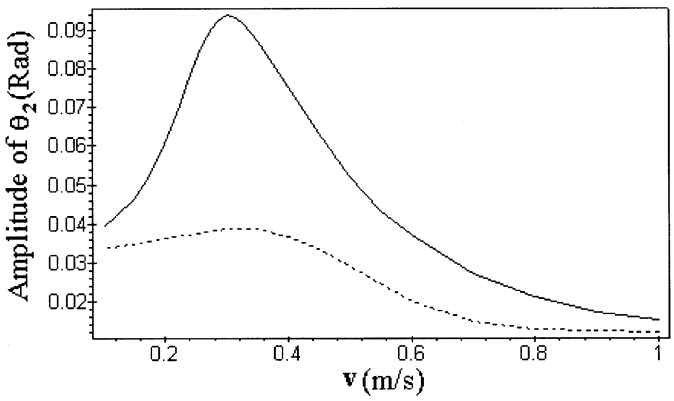

*Dashed: Without dynamic interaction effects, **Solid:** With dynamic interaction effects

Fig. 16. Amplitude of θ_2 versus velocity of vehicle*

VII. CONCLUSIONS

The kinematics and dynamics modeling of a two-degrees-of-freedom manipulator attached to a vehicle with a two-degrees-of-freedom suspension system is presented. It is shown that if the manipulator's joint positions, velocities and accelerations (i.e. θ_1, $\dot{\theta}_1$, $\ddot{\theta}_1$, θ_2, $\dot{\theta}_2$, $\ddot{\theta}_2$) are known as a function of time, the differential equations of motion of vehicle and manipulator will appear as a set of ordinary differential equations. In this case the forces and torque exerted to the vehicle by the manipulator act as a known input. For the case where the manipulator is to follow a straight line trajectory with a constant tracking speed, it is required to compute the value of θ_1, $\dot{\theta}_1$, $\ddot{\theta}_1$, θ_2, $\dot{\theta}_2$ and $\ddot{\theta}_2$ such that the end effector follow the desired trajectory. In this case, parameters y, ψ, θ_1, θ_2 will appear as a functions of each other. As a result, the differential equations of motion will be a set of partial differential equations. To avoid this situation, a numerical method has been presented. With the aforementioned procedure one can solve the said ordinary differential equations without converting them into partial differential equations. These results can be used for designing the parameters of a vehicle and its suspension system, and also as a guideline for choosing the control strategy.

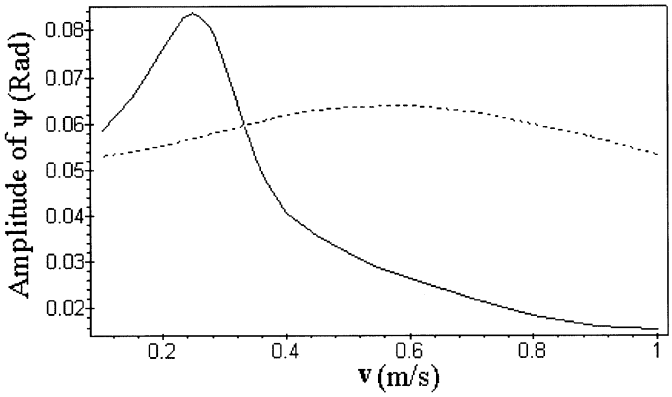

*Dashed: Without dynamic interaction effects, **Solid:** With dynamic interaction effects

Fig. 14. Amplitude of ψ versus velocity of vehicle*

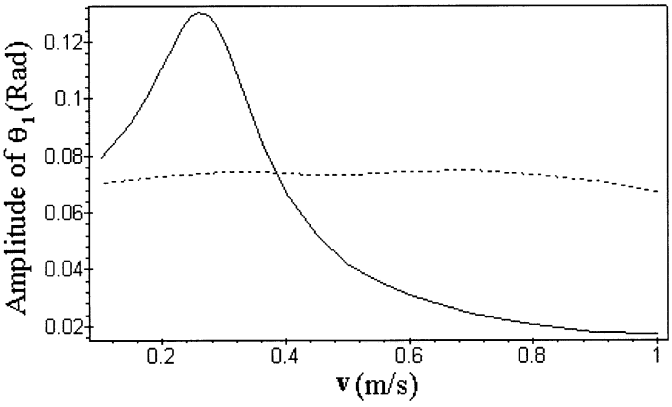

*Dashed: Without dynamic interaction effects, **Solid:** With dynamic interaction effects

Fig. 15. Amplitude of θ_1 versus velocity*

References

1. U.M. Nassal, "Motion Coordination and Reactive Control of Autonomous Multi-Manipulator System", *J. of Robotic Systems* **13**, No. 11, 737–754 (1996).
2. S. Dubowsky and E.E. Vance, "Planning Mobile Manipulator Motion Considering Vehicle Dynamic Stability Constraints," *Proc. of the IEEE Conf. on Robotics and Automation* (1989), **Vol. 3**, pp. 1271–1276.
3. E.G. Paradopoulos and D.A. Rey, "New Measure of Tipover Stability Margin for Mobile Manipulators", *Proc. of the IEEE Conf. on Robotics and Automation*, **Vol. 4**, pp. 3111–3116 (1996).
4. M.W. Chen and A.M.S. Zalzala, "Dynamic Modelling and Genetic-Base Trajectory Generation for Nonholonomic Mobile Manipulators", *Control Engineering Practice* **5**, No. 1, 39–48 (1997).
5. Y. Yamamoto and X. Yun, "Effect of the Dynamic Interaction on Coordinated Control of Mobile Manipulators", *IEEE Trans. on Robotics and Automation* **12**, No. 5, 816–824 (1996).
6. F.G. Pin, K.A. Morgansen, F.A. Tulloch, C.J. Hacker and K.B. Gower, "Motion Planning for Mobile Manipulators with a Non-holonomic Constant Using the FSP Method," *J. Robotic Systems* **13**, No. 11, 723–736 (1996).
7. W.F. Carrikar, P.K. Khosla and B.H. Krogh, "Path Planning for Mobile Manipulators for Multiple Task Execution", *IEEE Trans. on Robotics and Automation* **7**, No. 3, 403–408 (1991).
8. N.A. Lakota, E.V. Rakhmanov, A.N. Shvedov and V.N. Strelkov, "Modelling of an Elastic Manipulator on Moving Base," *Scripta Technica, Inc.* 150–154 (1986).
9. Yoshio Yamamoto, Eda Hiroshi and Yun Xiaoping, "Coordinated Task Execution of a Human and a Mobile Manipulator,"

https://doi.org/10.1017/S0263574700003131 Published online by Cambridge University Press

Proc. of the IEEE Conf. on Robotics and Automation (1996), **Vol. 2**, pp. 1006–1011.
10. C.C. Wang and V. Kumar, "Velocity Control of Mobile Manipulator", *Proc. of the IEEE Conf. on Robotics and Automation* (1996), **Vol. 2**, pp. 713–718.
11. W. Oelen, H. Berghuits, H. Nijmeijer and C. Candasdewit, "Implementation of a Hybrid Stabilizing Controller on a Mobile Robot with Two Degrees of Freedom", *Proc. of the IEEE Conf. on Robotics and Automation* (1994), **Vol. 1**, pp. 1196–1201.
12. K.A. Tohboub, "Robust Control of Mobile Manipulators", *J. Robotic Systems*, **13**, No. 11, 699–708 (1996).
13. K.A. Tohboub, "On the Control of Mobile Manipulators", *Proc. of the World Automation Congress* (1998) **Vol. 7**, pp. 307–312.
14. A. Meghdari, M. Durali and D. Naderi, "Dynamic Interaction Between the Manipulator and vehicle of a mobile manipulator", *Proc. of 1999 ASME International Mechanical Engineering Congress*, Nashville, TN, USA (Nov. 14–19, 1999) **Vol. DE 101**, pp. 61–67.
15. D.C. Cole, "Front-Rear Interaction of a Pitch-Plan Truck Model", *J. Vehicle System Dynamics* **30**, 117–141 (1998).
16. J.J. Craig, *Introduction to Robotics; Mechanics and Control*, 2nd ed. (Addison-Wesley 1989).

NOMENCLATURE

Distance between rear and front axles	a
Distance between rear axle and mass center of vehicle	b
Components of position vector locating the origin of frame {0} in frame {B}	{c,e}
Damper coefficient of rear damper	C_1
Damper coefficient of front damper	C_2
Traction force of rear wheel	f
First natural frequency of vehicle	f_{n1}
Second natural frequency of vehicle	f_{n2}
Inertial force acting at the center of mass of link in frame {i}	${}^{i}F_i$
Force exerted on link i by link i-1 in frame {j}	${}^{j}f_i$
Gravitational constant	g
The central inertial tensor for vehicle	I_G
The central inertial tensor for link i	${}^{c_i}I_i$
Spring coefficient of rear spring	k_1
Spring coefficient of front spring	k_2
Length of the link i	ℓ_i
Mass of the link i	m_i
Mass of the vehicle	m_B
Inertial torque acting at the center of mass of link i in frame {i}	${}^{i}N_i$
Torque exerted on link i by link i-1 in frame {i}	${}^{i}n_i$
Position vector locating the mass center of link i in frame {i}	${}^{i}p_{c_i}$
Rotation matrix of frame {i} relative to frame {j}	${}^{j}_{i}R$
Time	t
Homogeneous transformation matrix of frame {i} relative to frame {j}	${}^{j}_{i}T$
Speed of vehicle	v
Tracking speed	v_f
Linear acceleration of the origin of frame {i} in frame {i}	${}^{i}\dot{v}_i$
Linear acceleration of mass center of the link i in frame {i}	${}^{i}\dot{v}_{c_i}$
The horizontal coordinate of the end-effector's position in frame {S}	${}^{S}X$
Unit vector in the direction of X_i	$\hat{X}_i$
Vertical displacement of mass center of vehicle in frame {S}	y
The vertical coordinate of the end-effector's position in frame {S}	${}^{S}Y$
Unit vector in the direction of Z_i in frame {i}	${}^{i}\hat{Z}_i$
Constant denoting the slope of the trajectory line equation	α
Constant of the trajectory line equation	β
The angle between X_{i-1} and X_i measured about Z_i	θ_i
Torque of the ith Actuator	τ_i
Rotation of vehicle in frame {S}	ψ
Angular velocity of link in frame {i}	${}^{i}\omega_i$

APPENDIX A

$$ {}^{1}\omega_1 = {}^{1}_{0}R\,{}^{0}\omega_0 + \dot{\theta}_1\,{}^{1}\hat{Z}_1 \quad , \quad {}^{1}\omega_1 = \dot{\theta}_1\,{}^{1}\hat{Z}_1 = \begin{bmatrix} 0 \\ 0 \\ \dot{\psi} + \dot{\theta}_1 \end{bmatrix} \tag{A-1} $$

$$ {}^{1}\dot{\omega}_1 = {}^{1}_{0}R\,{}^{0}\dot{\omega}_0 + {}^{1}_{0}R\,{}^{0}\omega_0 \times \dot{\theta}_1\,{}^{1}\hat{Z}_1 + \ddot{\theta}_1\,{}^{1}\hat{Z}_1 \quad , \quad {}^{1}\dot{\omega}_1 = \ddot{\theta}_1\,{}^{1}\hat{Z}_1 = \begin{bmatrix} 0 \\ 0 \\ \ddot{\psi} + \ddot{\theta}_1 \end{bmatrix} \tag{A-2} $$

$$ {}^{1}\dot{v}_1 = {}^{1}_{0}R\left({}^{0}\dot{\omega}_0 \times {}^{0}P_1 + {}^{0}\omega_0 \times \left({}^{0}\omega_0 \times {}^{0}P_1\right) + {}^{0}\dot{v}_0\right) \tag{A-3} $$

$$ {}^{1}\dot{v}_1 = \begin{bmatrix} h\ddot{\psi}\sin(\theta_1 - \gamma) - h\dot{\psi}^2\cos(\theta_1 - \gamma) + (g + \ddot{y})\sin(\theta_1 + \psi) \\ h\ddot{\psi}\cos(\theta_1 + \gamma) + h\dot{\psi}^2\sin(\theta_1 - \gamma) + (g + \ddot{y})\cos(\theta_1 + \psi) \\ 0 \end{bmatrix} \tag{A-4} $$

$$ {}^{1}\dot{v}_{c_1} = {}^{1}\dot{\omega}_1 \times {}^{1}P_{c_1} + {}^{1}\omega_1 \times \left({}^{1}\omega_1 \times {}^{1}P_{c_1}\right) + {}^{1}\dot{v}_1 \tag{A-5} $$

$$ {}^{1}\dot{v}_{c_1} = \begin{bmatrix} -\ell_1/2(\dot{\psi} + \dot{\theta}_1)^2 + h\ddot{\psi}\sin(\theta_1 - \gamma) - h\dot{\psi}^2\cos(\theta_1 - \gamma) + (g + \ddot{y})\sin(\theta_1 + \psi) \\ \ell_1/2(\ddot{\psi} + \ddot{\theta}_1) + h\ddot{\psi}\cos(\theta_1 - \gamma) + h\dot{\psi}^2\sin(\theta_1 - \gamma) + (g + \ddot{y})\cos(\theta_1 + \psi) \\ 0 \end{bmatrix} \tag{A-6} $$

$$ {}^{1}F_1 = m_1\,{}^{1}\dot{v}_{c_1} \tag{A-7} $$

$$ {}^{1}F_1 = \begin{bmatrix} -m_1\ell_1/2(\dot{\psi} + \dot{\theta}_1)^2 + m_1h\ddot{\psi}\sin(\theta_1 - \gamma) - m_1h\dot{\psi}^2\cos(\theta_1 - \gamma) + m_1(g + \ddot{y})\sin(\theta_1 + \psi) \\ m_1\ell_1/2(\ddot{\psi} + \ddot{\theta}_1) + m_1h\ddot{\psi}\cos(\theta_1 - \gamma) + m_1h\dot{\psi}^2\sin(\theta_1 - \gamma) + m_1(g + \ddot{y})\cos(\theta_1 + \psi) \\ 0 \end{bmatrix} \tag{A-8} $$

$$ {}^{1}N_1 = {}^{c_1}I_1\,{}^{1}\dot{\omega}_1 + {}^{1}\omega_1 \times {}^{c_1}I_1\,{}^{1}\omega_1 \quad , \quad {}^{1}N_1 = \begin{bmatrix} 0 \\ 0 \\ 0 \end{bmatrix} \tag{A-9} $$

https://doi.org/10.1017/S0263574700003131 Published online by Cambridge University Press

$$ {}^2\omega_2 = {}^2_1R\,{}^1\omega_1 + \dot\theta_2\,{}^2\hat Z_2 \qquad , \qquad {}^2\omega_2 = \begin{bmatrix} 0 \\ 0 \\ \dot\psi + \dot\theta_1 + \dot\theta_2 \end{bmatrix} \tag{A-10} $$

$$ {}^2\dot\omega_2 = {}^2_1R\,{}^1\dot\omega_1 + {}^2_1R\,{}^1\omega_1 \times \dot\theta_2\,{}^2\hat Z_2 + \ddot\theta_2\,{}^2\hat Z_2 \quad , \quad {}^2\omega_2 = \begin{bmatrix} 0 \\ 0 \\ \ddot\psi + \ddot\theta_1 + \ddot\theta_2 \end{bmatrix} \tag{A-11} $$

$$ {}^2\dot v_2 = {}^2_1R({}^1\dot\omega_1 \times {}^1P_2 + {}^1\omega_1 \times ({}^1\omega_1 \times {}^1P_2) + {}^1\dot v_1) \tag{A-12} $$

$$ {}^2\dot v_2 = \begin{bmatrix} -\ell_1(\dot\psi+\dot\theta_1)^2\cos(\theta_2) + \ell_1(\ddot\psi+\ddot\theta_1)\sin(\theta_2) \\ -h\dot\psi^2\cos(\theta_1+\theta_2-\gamma) + h\ddot\psi\sin(\theta_1+\theta_2-\gamma) \\ +(g+\ddot y)\sin(\theta_1+\theta_2+\psi) \\ \\ \ell_1(\dot\psi+\dot\theta_1)^2\sin(\theta_2) + \ell_1(\ddot\psi+\ddot\theta_1)\cos(\theta_2) \\ +h\dot\psi^2\sin(\theta_1+\theta_2-\gamma) + h\ddot\psi\cos(\theta_1+\theta_2-\gamma) \\ +(g+\ddot y)\cos(\theta_1+\theta_2+\psi) \\ \\ 0 \end{bmatrix} \tag{A-13} $$

$$ {}^2\dot v_{c_2} = {}^2\dot\omega_2 \times {}^2P_{c_2} + {}^2\omega_2 \times \left({}^2\omega_2 \times {}^2P_{c_2}\right) + {}^2\dot v_2 \tag{A-14} $$

$$ {}^2\dot v_{c_2} = \begin{bmatrix} \ell_1(\ddot\psi+\ddot\theta_1)\sin(\theta_2) - \ell_1(\dot\psi+\dot\theta_1)^2\cos(\theta_2) \\ -\ell_2/2(\dot\psi+\dot\theta_1+\dot\theta_2)^2 - h\dot\psi^2\cos(\theta_1+\theta_2-\gamma) \\ +h\ddot\psi\sin(\theta_1+\theta_2-\gamma) + (g+\ddot y)\sin(\theta_1+\theta_2+\psi) \\ \\ \ell_1(\ddot\psi+\ddot\theta_1)\cos(\theta_2) + \ell_1(\dot\psi+\dot\theta_1)^2\sin(\theta_2) \\ \ell_2/2(\ddot\psi+\ddot\theta_1+\ddot\theta_2) + h\dot\psi^2\sin(\theta_1+\theta_2-\gamma) \\ +h\ddot\psi\cos(\theta_1+\theta_2-\gamma) + (g+\ddot y)\cos(\theta_1+\theta_2+\psi) \\ \\ 0 \end{bmatrix} \tag{A-15} $$

$$ {}^2F_2 = m_2\,{}^2\dot v_{c_2} \tag{A-16} $$

$$ {}^2N_2 = {}^{c_2}I_2\,{}^2\dot\omega_2 + {}^2\omega_2 \times {}^{c_2}I_2\,{}^2\omega_2 \qquad \Rightarrow \qquad {}^2N_2 = \begin{bmatrix} 0 \\ 0 \\ 0 \end{bmatrix} \tag{A-17} $$

$$ {}^2f_2 = {}^2_3R\,{}^3f_3 + {}^2F_2 \qquad \Rightarrow \qquad {}^2f_2 = {}^2F_2 \tag{A-18} $$

$$ {}^2n_2 = {}^2N_2 + {}^2_3R\,{}^3n_3 + {}^2P_{c_2} \times {}^2F_2 + {}^2P_3 \times {}^2_3R\,{}^3f_3 \quad , \quad {}^2n_2 = \begin{bmatrix} 0 \\ 0 \\ \tau_2 \end{bmatrix} \tag{A-19} $$

$$ \begin{aligned} \tau_2 = {} & m_2\ell_1\ell_2/2(\ddot\psi+\ddot\theta_1)\cos(\theta_2) + m_2\ell_1\ell_2/2(\dot\psi+\dot\theta_1)^2\sin(\theta_2) \\ & + m_2\ell_2^2/4(\ddot\psi+\ddot\theta_1+\ddot\theta_2) + m_2h\ell_2/2\ddot\psi\cos(\theta_1+\theta_2-\gamma) \\ & - m_2h\ell_2/2\dot\psi^2\sin(\theta_1+\theta_2-\gamma) \\ & + m_2\ell_2/2(g+\ddot y)\cos(\theta_1+\theta_2+\psi) \end{aligned} \tag{A-20} $$

$$ {}^1f_1 = {}^1_2R\,{}^2f_2 + {}^1F_1 \tag{A-21} $$

$$ {}^1f_1 = \begin{bmatrix} -m_1\ell_1/2(\dot\theta_1+\dot\psi)^2 - (m_1+m_2)h\dot\psi^2\cos(\theta_1-\gamma) \\ +(m_1+m_2)h\ddot\psi\sin(\theta_1-\gamma) \\ +(m_1+m_2)(g+\ddot y)\sin(\theta_1+\psi) \\ -m_2\ell_2/2(\dot\theta_1+\dot\theta_2+\dot\psi)^2\cos\theta_2 \\ -m_2\ell_2/2(\ddot\theta_1+\ddot\theta_2+\ddot\psi)\sin\theta_2 - m_2\ell_1(\dot\theta_1+\dot\psi)^2 \\ \\ -m_1\ell_1/2(\ddot\theta_1+\ddot\psi) + (m_1+m_2)h\dot\psi^2\sin(\theta_1-\gamma) \\ +(m_1+m_2)h\ddot\psi\cos(\theta_1-\gamma) \\ +(m_1+m_2)(g+\ddot y)\cos(\theta_1+\psi) \\ -m_2\ell_2/2(\dot\theta_1+\dot\theta_2+\dot\psi)^2\sin\theta_2 \\ +m_2\ell_2/2(\ddot\theta_1+\ddot\theta_2+\ddot\psi)\cos\theta_2 + m_2\ell_1(\ddot\theta_1+\ddot\psi) \\ \\ 0 \end{bmatrix} \tag{A-22} $$

$$ {}^1n_1 = {}^1N_1 + {}^1_2R\,{}^2n_2 + {}^1P_{c_1} \times {}^1F_1 + {}^1P_2 \times {}^1_2R\,{}^2f_2 \quad , \quad {}^1n_1 = \begin{bmatrix} 0 \\ 0 \\ \tau_1 \end{bmatrix} \tag{A-23} $$

$$ {}^0f_1 = {}^0_1R\,{}^1f_1 \qquad , \qquad {}^0f_1 = \begin{bmatrix} f_x \\ f_y \\ 0 \end{bmatrix} \tag{A-24} $$

https://doi.org/10.1017/S0263574700003131 Published online by Cambridge University Press